ISSN 1063-7796, Physics of Particles and Nuclei, 2021, Vol. 52, No. 4, pp. 555–559. © Pleiades Publishing, Ltd., 2021.

Holographic Model for Light Quarks in Anisotropic Background

K. A. Rannu*

Peoples Friendship University of Russia, Moscow, 117198 Russia

**e-mail: rannu-ka@rudn.ru*

Received October 20, 2020; revised November 23, 2020; accepted November 23, 2020

Abstract—We present a five-dimensional holographic model for light quarks in hot dense anisotropic QGP, that is an expansion of our previous anisotropic solution [1, 2]. AdS_5 black hole solution of EOM is obtained, its thermodynamic properties are discussed. Confinement/deconfinement phase diagram is constructed.

DOI: 10.1134/S1063779621040511

1. INTRODUCTION

In the holographic approach [3–5] to describe hot dense anisotropic quark-gluon plasma (QGP), produced in heavy-ion collisions (HIC) [6, 7], we use the following action and metric ansatz:

$$S = \frac{1}{16\pi G_5}\int d^5x\sqrt{-g} \times\left[R - \frac{f_1(\phi)}{4}F_{(1)}^2 - \frac{f_2(\phi)}{4}F_{(2)}^2 - \frac{1}{2}\partial_\mu\phi\partial^\mu\phi - V(\phi)\right], \quad \text{(I.1)}$$

$$ds^2 = \frac{L^2}{z^2}\mathfrak{b}(z) \times\left[-g(z)dt^2 + dx^2 + \left(\frac{z}{L}\right)^{2-\frac{2}{\nu}}dy_1^2 + \left(\frac{z}{L}\right)^{2-\frac{2}{\nu}}dy_2^2 + \frac{dz^2}{g(z)}\right], \quad \text{(I.2)}$$

where 5-dim coordinates describe the energy scale of the process that we consider.

In Eq. (1.1), the Maxwell field $F_{\mu\nu}^{(1)} = \partial_\mu A_\nu - \partial_\nu A_\mu$ is set by $A_\mu^{(1)} = A_t(z)\delta_\mu^0$ and serves to introduce the chemical potential μ describing the baryonic density. The other Maxwell field $F_{\mu\nu}^{(2)} = qdy^1 \wedge dy^2$ is needed to support the anisotropy of the solution along the **y** directions as opposed to the x direction. This anisotropy parametrized by ν describes the spacial anisotropy of the QGP produced in HIC. Coupling functions $f_1(\phi)$ and $f_2(\phi)$ are associated with the Maxwell fields $F_{\mu\nu}^{(1)}$ and $F_{\mu\nu}^{(2)}$, respectively, $\phi = \phi(z)$ is the scalar field and $V(\phi)$ is the scalar field potential.

In the metric (1.2), $g(z)$ is the blackening function and $\mathfrak{b}(z)$ is the warp factor. The form of the warp-factor determines the quark mass that is considered in the model. In our previous works [1, 2] we used the warp-factor $\mathfrak{b}(z) = e^{-cz^2}$, thus investigating the holographic model for heavy quarks (b, t). This time we follow [8] and take

$$\mathfrak{b}(z) = e^{2\mathcal{A}(z)}, \quad \mathcal{A}(z) = -a\ln(bz^2+1), \quad \text{(I.3)}$$

that allows us to study light quarks' (d, u) behavior, and in all numerical calculations we admit $L = 1$, $a = 4.046$, $b = 0.01613$, $c = 0.227$ [9].

You can learn more on motivation, reasoning and methods of the holographic approach in talk by Aref'eva from this conference [10].

2. SOLUTION

To solve the EOM derived from (I.1) and satisfying the ansatz (I.2) we assume $f_1 = e^{-cz^2-A(z)}z^{-2+\frac{2}{\nu}}$ and take the boundary conditions

$$A_t(0) = \mu, \quad A_t(z_h) = 0, \quad g(0) = 1, \quad g(z_h) = 0, \quad \varphi(z_0) = 0, \quad \text{(II.1)}$$

where z_h is the horizon size and z_0 is the boundary condition point, $(0 \le z_0 \le z_h)$.

For light quarks we get the following solution:

$$A_t = \mu\frac{e^{cz^2} - e^{cz_h^2}}{1 - e^{cz_h^2}}, \quad \text{(II.2)}$$

$$g = 1 - \frac{\int_0^z \left(1+b\xi^2\right)^{3a}\xi^{1+\frac{2}{\nu}}d\xi}{\int_0^{z_h}\left(1+b\xi^2\right)^{3a}\xi^{1+\frac{2}{\nu}}d\xi} + \frac{2\mu^2 c}{L^2\left(1-e^{cz_h^2}\right)^2}\int_0^z e^{c\xi^2}\left(1+b\xi^2\right)^{3a}\xi^{1+\frac{2}{\nu}}d\xi\left[1 - \frac{\int_0^z \left(1+b\xi^2\right)^{3a}\xi^{1+\frac{2}{\nu}}d\xi}{\int_0^{z_h}\left(1+b\xi^2\right)^{3a}\xi^{1+\frac{2}{\nu}}d\xi}\frac{\int_0^{z_h} e^{c\xi^2}\left(1+b\xi^2\right)^{3a}\xi^{1+\frac{2}{\nu}}d\xi}{\int_0^z e^{c\xi^2}\left(1+b\xi^2\right)^{3a}\xi^{1+\frac{2}{\nu}}d\xi}\right], \quad \text{(II.3)}$$

$$f_2 = -\left(\frac{z}{L}\right)^{1-\frac{4}{\nu}} \frac{e^{2\mathcal{A}}}{Lq^2}\left[2g'\frac{\nu-1}{\nu} + 6g\frac{\nu-1}{\nu}\left(\mathcal{A}' - \frac{2(\nu+1)}{3\nu z}\right)\right], \tag{II.4}$$

$$\phi = \int_{z_0}^{z} \frac{2\sqrt{\nu - 1 + \left(2(\nu-1) + 9a\nu^2\right)b\xi^2 + \left(\nu - 1 + 3a(1+2a)\nu^2\right)b^2\xi^4}}{(1+b\xi^2)\nu\xi} d\xi, \tag{II.5}$$

$$V = -\frac{3gz^2 e^{-2A}}{L}\left[\mathcal{A}'' + 3\mathcal{A}'^2 + \left(\frac{3}{2}\frac{g'}{g} - \frac{3(\nu+1)}{\nu z}\right)\mathcal{A}' - \frac{1}{\nu z}\left(\frac{4+5\nu}{6}\frac{g'}{g} - \frac{2(\nu+1)(2\nu+1)}{3\nu z}\right) + \frac{g''}{6g}\right]. \tag{II.6}$$

An important feature of the solution is that in the anisotropic case $\nu > 1$ we have logarithmic divergence if the dilaton, $\phi(z) \sim \int_0^z dz/z$, for $z_0 = 0$. To establish a smooth connection to the isotropic case we can use a small enough, but non-zero value of z_0. More details on purposes and sequences of a boundary condition choice for the scalar field are discussed in the talk by P. Slepov from this conference [11].

3. THERMODYNAMICS

3.1. Temperature and Entropy

For the metric (1.2) and the chosen warp-factor, the temperature can be written as:

$$T = \frac{|g'|}{4\pi}\Big|_{z=z_h}$$

$$= \frac{1}{4\pi}\left|-\frac{\left(1+bz_h^2\right)^{3a} z_h^{1+\frac{2}{\nu}}}{\int_0^{z_h}\left(1+b\xi^2\right)^{3a}\xi^{1+\frac{2}{\nu}}d\xi}\left[1 - \frac{2\mu^2 c e^{2cz_h^2}}{L^2\left(1-e^{cz_h^2}\right)^2}\right.\right.$$

$$\times\left(1 - e^{-cz_h^2}\frac{\int_0^{z_h} e^{c\xi^2}\left(1+b\xi^2\right)^{3a}\xi^{1+\frac{2}{\nu}}d\xi}{\int_0^{z_h}\left(1+b\xi^2\right)^{3a}\xi^{1+\frac{2}{\nu}}d\xi}\right) \tag{III.1}$$

$$\left.\left. \times \int_0^{z_h}\left(1+b\xi^2\right)^{3a}\xi^{1+\frac{2}{\nu}}d\xi\right]\right|.$$

In the isotropic case for $\mu = 0$ the temperature is a monotonically decreasing function of horizon (Fig. 1a). For nonzero chemical potential, $T(z_h)$ becomes a three-digit function. Its local minimum value is lesser for larger μ. Finally it reaches zero and a second horizon appears. In the isotropic case this happens at $\mu \approx 0.557$. In the anisotropic case, the temperature is a three-digit function even for $\mu = 0$. As for the second horizon, it appears at about $\mu \approx 0.852$ for $\nu = 1.5$ (Fig. 1b), $\mu \approx 1.218$ for $\nu = 3$ (Fig. 1c) and $\mu \approx 1.336$ for $\nu = 4.5$ (Fig. 1d).

As it is shown below, these features of the temperature determine the phase diagram, so that in anisotropic cases we have the Hawking–Page-like (BB) phase transition line for zero μ (Fig. 1b).

For (1.2) and the chosen warp-factor, the entropy becomes

$$s = \left(L/z_h\right)^{1+\frac{2}{\nu}}\left(1+bz_h^2\right)^{-3a}/4. \tag{III.2}$$

It decreases monotonocally and quickly with horizon growth (Fig. 2a).

3.2. Free Energy and Phase Diagram

To get the Hawking–Page-like transition line we need to consider the free energy as a function of temperature:

$$F = \int_{z_h}^{z_{h_2}} sT'\,dz, \tag{III.3}$$

where $z_{h_2} = \infty$ for $T \geq 0$ and z_{h_2} is the second horizon for $T = 0$: $z_{h_2} = 4.609$ for $\nu = 1$, $\mu = 0.557$, $z_{h_2} = 4.163$ for $\nu = 1.5$, $\mu = 0.852$ and $z_{h_2} = 3.102$ for $\nu = 4.5$, $\mu = 1.336$.

For the Hawking–Page-like phase transition the free energy should be a multi-valued function of temperature. Graphically it is displayed as a swallow-tail. The point where the free energy curve corresponding to some μ intersects itself (or the T-axis) determines the temperature of the Hawking–Page-like phase transition for this μ.

In Fig. 3 the function $F(T)$ for zero chemical potential and different ν is shown. For $1 \leq \nu \leq 1.04$ the free energy lies in the lower half-plane without any self-intersection, therefore the Hawking–Page-like phase transition for $\mu = 0$ exists. For $\nu = 1.05$ an obtuse angle—a germ of the swallow-tail—appears. Further anisotropy growth makes the swallow-tails more pronounced. On the other hand, increasing the anisotropy from 1 to 1.04 shifts the critical point to the left towards the T-axis, so the gap between them narrows and quickly—when $\nu = 1.05$—closes. Starting from this moment, the Hawking–Page transition line exists for all chemical potential values $0 \leq \mu \leq \mu_{max}$.

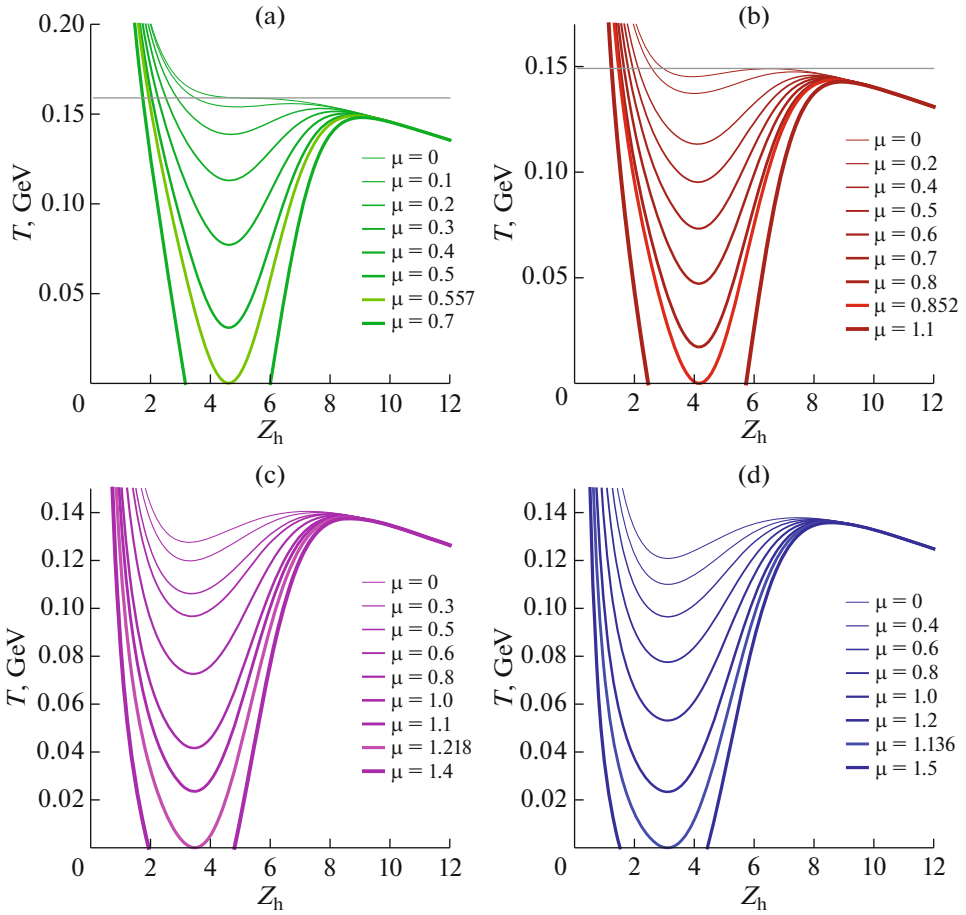

Fig. 1. Temperature as function of horizon for different μ in isotropic (a) and anisotropic cases for ν = 1.5 (b), ν = 3 (c), ν = 4.5 (d); $a = 4.046$, $b = 0.01613$, $c = 0.227$.

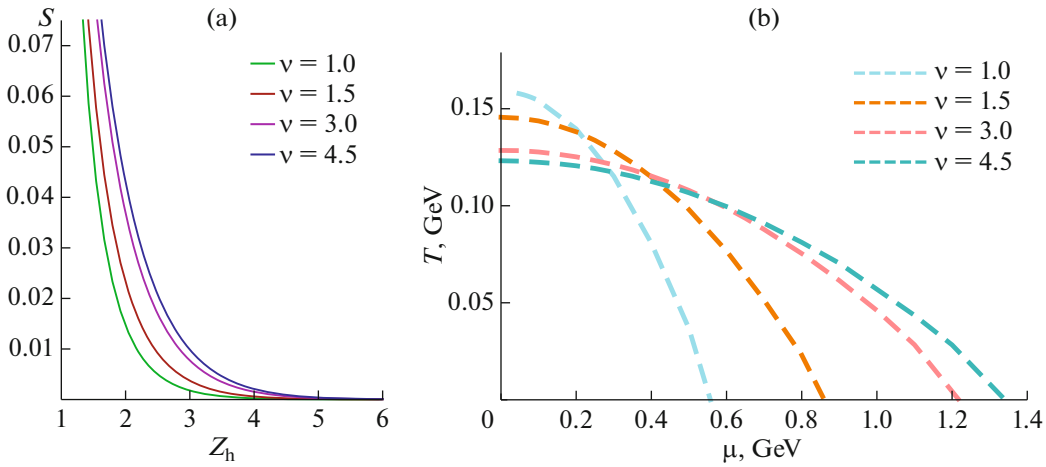

Fig. 2. Entropy as function of horizon (a) and Hawking–Page-like-phase transition lines $T(\mu)$ for isotropic (ν = 1) and anisotropic (ν = 1.5, 3, 4.5) cases (b); $a = 4.046$, $b = 0.01613$, $c = 0.227$.

Figure 2b shows the Hawking–Page-like phase transition lines for ν = 1, 1.5, 3, 4.5. In the isotropic case, the BB-phase transition starts from a critical point $\mu_c = 0.04779$, $T_c = 0.1578$ that fully coincides with the previous result in [8]. One can see that isotropisation leads to smaller chemical potential values, but the temperature for given μ rises.

To get the full picture of the confinement/deconfinement phase transition we also need to consider temporal Wilson loops that depend on the quark pair

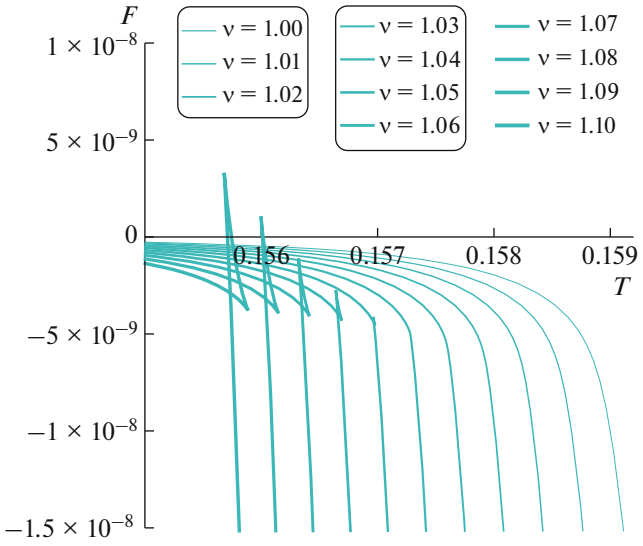

Fig. 3. Free energy as function of temperature $F(T)$ for $\mu = 0$ in isotropic ($\nu = 1$) and slightly anisotropic ($\nu = 1.01, 1.02, 1.03, 1.04, 1.05, 1.06, 1.07, 1.08, 1.09, 1.1$) cases; $a = 4.046$, $b = 0.01613$, $c = 0.227$.

orientation. As the current model differs from the previous one by the form of the warp-factor only, all the reasoning in [1, 2] remains applicable here. Therefore, the dynamical wall equations become:

$$-\frac{4abz}{1+bz^2}+\sqrt{\frac{2}{3}}\phi'+\frac{g'}{2g}=\frac{2}{z},$$
$$-\frac{4abz}{1+bz^2}+\sqrt{\frac{2}{3}}\phi'+\frac{g'}{2g}=\frac{\nu+1}{\nu z} \qquad \text{(III.4)}$$

for longitudinal (x) and transversal ($\mathbf{y}$) direction correspondingly.

In Fig. 4a the isotropic case is depicted. The confinement/deconfinement phase transition is mostly determined by the Hawking–Page-like transition (BB-transition). Wilson loop is sufficient in a small region of crossover for $0 < \mu < 0.104$, i.e. till the point (0.104, 0.153), where two phase transition lines intersect.

In the anisotropic case, the isotropic Wilson line splits into two. The line corresponding to the longitudinal Wilson loop lies above the Hawking–Page-like line and does not actually influence the phase transition. For larger anisotropy, the longitudinal Wilson line has lower temperature values, but the difference between it and the Hawking–Page-like line increases with ν (Figs. 4a–4d). The phase transition line corresponding to the transversal Wilson loop almost coincides with the Hawking–Page-like line, so there is no evident crossover region as seen in the anisotropic case. Therefore, the influence of the transversal Wilson line and the Hawking–Page-like line on the con-

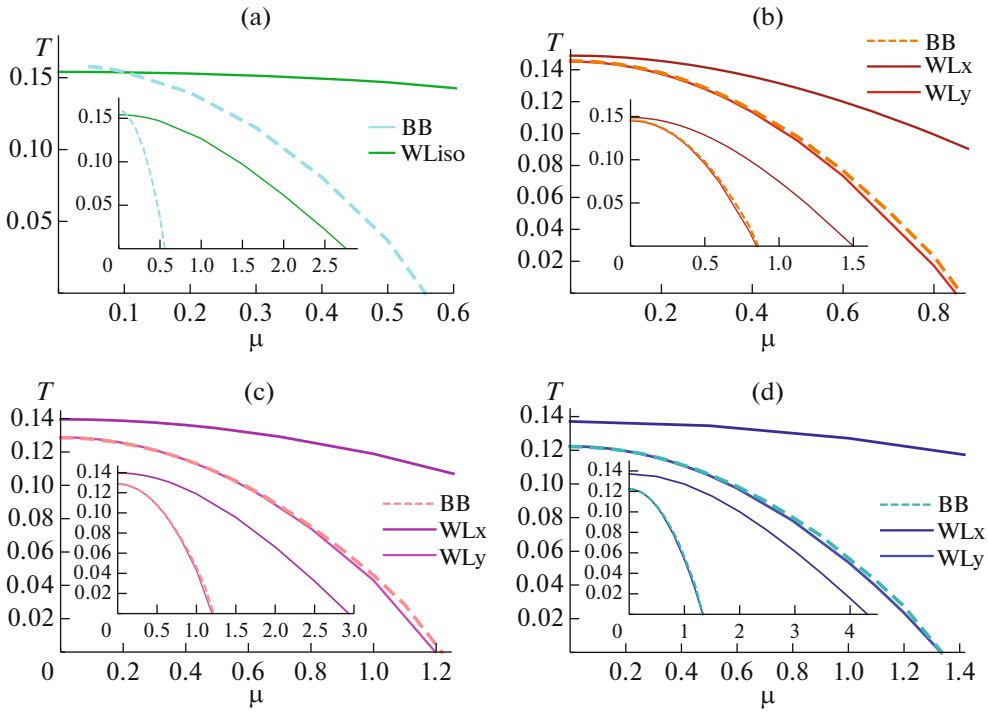

Fig. 4. Confinement/deconfinement phase diagram $T(\mu)$ in isotropic (a) and anisotropic cases for $\nu = 1.5$ (b), $\nu = 3$ (c), $\nu = 4.5$ (d); $a = 4.046$, $b = 0.01613$, $c = 0.227$. Dashed lines show Hawking–Page-like phase transitions (BB).

finement-deconfinement phase transition could be hardly distinguished from each other.

4. CONCLUSIONS

In this work a holographic model for light quarks is constructed. The 5-dim solution, describing hot dense anisotropic QCD within the AdS_5/CFT_4 duality was obtained. Peculiar thermodynamics properties of the solution that influence the confinement/deconfinement phase diagram are investigated.

Unlike the heavy quark model [1], the Hawking–Page-like phase transition line does not break at a relatively high temperature but lasts till $T = 0$. The main role transfers from it to the transversal Wilson loop with anisotropy growth. This transfer goes smoothly, without jumps that took place on the heavy quark phase diagram [1]. The longitudinal Wilson loop does not actually take part in the picture of confinement/deconfinement phase transition for light quarks.

As for further investigations, we plan to obtain a more realistic, hybrid model, where both heavy and light quarks would be included. The study of such a mix should promote better understanding of the confinement/deconfinement phase transition and interpretations of experimental data in future. We also plan to study an HQCD model in an external magnetic field by constructing a fully anisotropic solution, similar to what has been done in [12].

We hope that the results presented in this paper and their further possible adjustment to the phenomenological data can be of interest for experiments at the future facilities of FAIR, NICA, for the RHIC's BES II program and CERN, III run.

FUNDING

This work was supported by grant no. 18-02-40069 from the Russian Foundation for Basic Research.

REFERENCES

1. I. Ya. Aref'eva and K. Rannu, JHEP, No. **05**, 206 (2018).
2. I. Ya. Aref'eva, K. Rannu, and P. Slepov, Phys. Lett. B **792**, 470 (2019).
3. J. Casalderrey-Solana, H. Liu, et al., *Gauge/String Duality, Hot QCD and Heavy Ion Collisions* (Cambridge Univ. Press, 2014).
4. I. Ya. Aref'eva, Phys. Usp. **57**, 527 (2014).
5. I. Ya. Aref'eva and A. A. Golubtsova, JHEP, No. 04, 011 (2015).
6. J. Adam et al. (ALICE Collab.), Phys. Rev. Lett. **116**, 222302 (2016).
7. G. Aad et al. (ATLAS Collab.), Phys. Lett. B **170**, 363 (2012).
8. M.-W. Li, Y. Yang, and P.-H. Yuan, Phys. Rev. D **96**, 066013 (2017).
9. I. Aref'eva, K. Rannu, and P. Slepov, "Holographic anisotropic model for light quarks with confinement-deconfinement phase transition," arXiv:2009.05562 [hep-th] (2020).
10. I. Ya. Aref'eva, "Theoretical studies of the formation and properties of quark-gluon matter under conditions of high baryon densities attainable at the NICA experimental complex," in *Proceedings of the Conference "RFBR Grants for NICA"* (Dubna, 2020).
11. P. Slepov, "A way to improve string tension dependence on temperature in holographic model," in *Proceedings of the Conference "RFBR Grants for NICA"* (Dubna, 2020).
12. U. Gürsoy, M. Järvinen, G. Nijs, and J. F. Pedraza, JHEP, No. 04, 071 (2019).